Article

Ultrasensitive Electrochemiluminescence Biosensor for MicroRNA Detection by 3D DNA Walking Machine Based Target Conversion and Distance-Controllable Signal Quenching and Enhancing

Ziqi Xu, Linli Liao, Yaqin Chai, Haijun Wang, and Ruo Yuan

Anal. Chem., **Just Accepted Manuscript** • DOI: 10.1021/acs.analchem.7b01409 • Publication Date (Web): 13 Jul 2017

Ultrasensitive Electrochemiluminescence Biosensor for MicroRNA Detection by 3D DNA Walking Machine Based Target Conversion and Distance-Controllable Signal Quenching and Enhancing

Ziqi Xu, Linli Liao, Yaqin Chai, Haijun Wang*, Ruo Yuan*

Key Laboratory of Luminescent and Real-Time Analytical Chemistry (Southwest University), Ministry of Education, College of Chemistry and Chemical Engineering, Southwest University, Chongqing 400715, PR China

* Corresponding author. Tel.: +86-23-68252277; Fax: +86-23-68253172.
E-mail address: hjwang@swu.edu.cn (H. J. Wang); yuanruo@swu.edu.cn (R. Yuan)

ABSTRACT:

In this study, an electrochemiluminescence (ECL) regenerated biosensor was reported to sensitively detect microRNA through 3D DNA walking machine and "on-off-super on" strategy. Firstly, 3D DNA walking machine with higher efficiency of payload releasing and superior signal amplification than those of the traditional DNA walking machine was initially introduced in ECL system for converting target microRNA to intermediate DNA and achieving significant signal amplification. Secondly, the distance between CdS:Mn quantum dots and Au nanoparticles was increased with the hybridization of intermediate DNA and Au nanoparticles modified S2, which weakened the energy transfer for ECL signal recovering and excited the surface plasma resonance for further enhancing the signal to construct the "on-off-super on" biosensor. Such an "on-off-super on" strategy not only reduced the ECL background signal but also increased the detection sensitivity. Impressively, the elaborate-designed biosensor could be regenerated by Lambda exonuclease hydrolyzing the intermediate DNA to make Au nanoparticles modified S2 recover to original hairpin structure. With the amazing signal amplification of 3D DNA walking machine and sensitive distance control of "on-off-super on" strategy, the biosensor showed an excellent performance for microRNA-141 detection with a low detection limit of 3.3 fM and could be applied to human prostate cancer cells analysis. Furthermore, this work established foundation to apply 3D Walker in ECL methodology and provided effective way for analysis of other microRNA or cancer cell.

KEYWORDS: electrochemiluminescent, microRNA, DNA walking machine, "on-off-super on" strategy.

INTRODUCTION:

Cancer, which caused the deaths of nearly 8.2 million human beings in 2012 with a rise year by year, has become the major cause of mortality.[1] It is well known that the specific expression of microRNA (miRNA) is interrelated with the occurrence, progression and tumorigenesis of cancer.[2,3] MiRNA-141, an endogenous and noncoding RNA with 22 nucleotides, is regarded as an important tumor marker for its high percentage expression in breast cancer, prostate cancer and other cancers.[4,5] As a consequence, the sensitive detection of miRNA-141 has become great significance for cancer diagnosis. Conventional methods such as quantitative reverse transcription polymerase chain reaction,[6] fluorescence,[7,8] and Northern blotting[9] have been employed for miRNAs detection, but the sensitivity and specificity of them are not satisfactory.[10] In order to diagnose the cancer more accurately, the ultrasensitive detection of miRNA-141 is still in high demand. Currently, electrochemiluminescence (ECL), which has been widely used in various areas of immunoassay, aptasensor, and other bioassay for its high stability, low background and broad detection range, is a promising method in biomarker analysis and early cancer detection.[11,12]

To improve the sensitivity of ECL detection, some nucleic acid amplification methods were employed such as rolling circle amplification[13,14] and polymerase chain reaction (PCR)[15,16] due to their signal enhancement capability. However, these methods not only have the strict reaction conditions and high demands for instruments and operations, but also might increase false positive or false negative signals. DNA walking machine, one of the artificial molecular machines which are constructed by smart synthetic DNA, has aroused an increasing interest for its efficient self-assembly nanostructure, cargoes handling capacity and imitative biological phenomena.[17,18] The nanostructure of DNA walking machine could be transformed

with the external stimuli such as energy-first DNA strands hybridization or the existence of ions, leading to cargoes transit and realizing targets detection. Nevertheless, the reports about DNA walking machines in recent years are limited in one dimensional (1D) or two dimensional (2D) nanostructure, and the effects of cargoes transit are unsatisfactory due to the inadequate ability of 1D or 2D walking space and low fluxes of the substrate DNA in nanostructures. Nowadays, 3D DNA walking machine has been newly reported to overcome the above shortages. All DNA components co-conjugated in a 3D space could provide a wide 3D track for walking and the high concentration of DNA components also could realize the rapid payload releasing and efficient enzymatic cleavage. Such a 3D DNA artificial molecular machine is an excellent construction in dynamic DNA nanotechnology which may bring a breakthrough to DNA nanodevices.[19] Significantly, the construction of 3D DNA walking machine is rarely studied in ECL methodology especially in cancer diagnosis until now.

Prior researches have shown that the "on-off-on" strategy is considered as a promising improvement method in quantitative determination with a wide detection range. Du and co-workers reported an "on-off-on" ECL sensor on account of the radical-scavenging of ethanol towards cobalt phthalocyanine decorated graphene oxide (GO–CoPc) to high sensitive detection of nonelectroactive organophosphate pesticides.[20] In previous work, we constructed an "on-off-on" ECL sensor based on the quenching to the ECL of N-(aminobutyl)-N-(ethylisoluminol) by mercury ion (Hg^{2+}) to sensitive detection of Hg^{2+} and mucin 1.[21] In those strategies, the obtained "on" state with a high ECL emission provided a prerequisite of ultrasensitive biodetection and then the obtained "off" state with a low ECL emission reduced the background signal and avoided the false positive signal. However, the

ECL signal of the second "on" state is not as high as that of the first "on" state, which limits the detection range and sensitivity of the biosensor. With this in mind, we hope to ameliorate the routine "on-off-on" strategy to further improve the sensitivity of the biosensor.

Herein, a novel ECL biosensor which combined with 3D DNA walking machine and "on-off-super on" strategy was constructed for ultrasensitive detection of miRNA. Au@Fe_3O_4 with the advantages of relatively large surface area and easy magnetic separation, was used to immobilize both walker probes and substrate probes to form the 3D DNA walking machine, which could achieve the conversion and amplification of target miRNA. As protecting probe paired with walker probe, the 3D DNA walking machine was locked and could not work. When the target miRNA existed, walker probe was released by the complementary pairing of target miRNA and protecting probe. Subsequently, walker probe paired with support probe to form the recognition site, and then was released again under the shearing of Nt.BsmAl nicking endonuclease. Therefore, the walker probe could match with another support probe, and then be released by Nt.BsmAI nicking endonuclease from near to far along the DNA-Au@Fe_3O_4 track. Due to the wide 3D walking space and high local concentration of DNA components, the 3D DNA walking machine resulted in an amazing amplification effect for target miRNA by generating a large number of intermediate DNAs. Secondly, the unique ECL performance of distance-based energy transfer between CdS:Mn quantum dots (QDs) and Au nanoparticles (AuNPs) was applied to construct an "on-off-super on" biosensors. When the classical luminescent CdS:Mn QDs existed alone on the sensing platform, there was a considerable ECL signal ("on" state). After introducing the Au nanoparticles modified S2 (AuNPs-S2), the ECL signal of the prepared CdS:Mn QDs was quenched by AuNPs

according to Förster energy transfer ("off" state). Afterward, the distance between AuNPs and CdS:Mn QDs was increased with the help of above intermediate DNA, which obtained a significant increasing ECL signal ("super on" state) due to the excited surface plasma resonance of AuNPs from CdS:Mn QDs comparing to the "on" state. Hence, the ECL signal produced by the excitation surface plasma resonance is stronger than that of the initial "on" state. Such an "on-off-super on" strategy based on ECL quenching and enhancing between AuNPs and CdS:Mn QDs not only afforded a high sensitive and wide range for miRNA detection, but also circumvented the false positive signal and the background signal. Lastly, Lambda exonuclease was used to degrade the intermediate DNA for recovering the hairpin shape of AuNPs-S2, by which the biosensor could be regenerated. This work extended the application of 3D DNA walking machine in the ECL field, and constructed an "on-off-super on" ECL regenerated biosensor for miRNA analysis, which may provide a sensitive and efficient way in early detection of cancers.

EXPERIMENTAL SECTION

Preparation of CdS:Mn QDs. The CdS:Mn quantum dots (QDs) were synthesized as follows. Briefly, $Cd(NO_3)_2 \cdot 4\ H_2O$ (0.1683 g) and $Mn(CH_3COO)_2 \cdot 4\ H_2O$ (0.0134 g) were dissolved in 30 mL ultrapure water and heated to 70 ºC under refluxing for 3 h. Following that, 30 mL freshly prepared Na_2S was added into the above mixture to obtain an orange precipitate immediately. Then, the CdS:Mn QDs were obtained after washing and centrifugation, storing at 4 ºC for later use.

Preparation of AuNPs-S2. A typical method for synthesizing AuNPs was added 0.6 mL ice cold $NaBH_4$ (0.1M) into 20 mL $HAuCl_4$ (0.25 mM), stirring the mixture until it turned to

orange-red. After centrifugation, the AuNPs were obtained. The hairpin DNA S2 was heated to 95 ºC for 5 min and then cooled to room temperature for 1 h before use. Later, 100 μL S2 (10 μM) was slowly added into the mixture which contained 500 μL AuNPs, 10 μL Tris-(2-carboxyethyl)-phosphine hydrochloride (TCEP, 10 mM) and 100 μL NaCl (0.5 M). After stirring in the dark for 16 h and centrifugation, the AuNPs-S2 was obtained and stored at 4 ºC for later use.

Preparation of intermediate DNA. The intermediate DNA was prepared by the following steps. Firstly, 500 μL NH_2-Fe_3O_4 was washed three times with ultrapure water and then added into the prepared 5mL AuNPs with stirring at 4 ºC for 1 h. After magnetically separating three times and redispersing into 1 mL PBS buffer, the Au@Fe_3O_4 was obtained. Meanwhile, 1 μL walker probe (1.5 μM) and 1 μL protecting probe (1.5 M) were mixed for 2 h at 37 ºC to form dsDNA. Then, 20 μL support probe (1.5 μM) was sufficiently mixed with the dsDNA and added into 20 μL Fe_3O_4@AuNPs, stirring overnight and magnetic separating to obtain the DNA-Au@Fe_3O_4. After that, 1 μL target miRNA-141 (1.5 μM) was added and completely paired with S3 for 2 h to release walker probe. Subsequently, the releasing walker probe paired with support probe, producing a recognition site for Nt.BsmAI which cut by 5U Nt.BsmAI nicking exonuclease at 37 ºC for 2 h to obtain an intermediate DNA and release walker probe again. Hence, a large number of intermediate DNA were obtained after magnetic separation.

Fabrication of the ECL biosensor. The fabrication of the ECL biosensor is showed in Scheme 1. Prior to use, the glassy carbon electrode (GCE) was polished with alumina powder and sonicated with ethanol and ultrapure water for 3 min in turn. After drying in the air, the

cleaned GCE was decorated by 20 μL CdS:Mn QDs and incubated overnight at room temperature to obtain the CdS:Mn QDs- film. Subsequently, 3-Mercaptopropionic acid (MPA) was modified with the CdS:Mn QDs for 5 h, and then EDC-NHS was used to activate carboxyl for 2 h. Then 20 μL S1 (1.5 μM) was incubated on the electrode at room temperature for 14 h ("on" state). After rinsing with ultrapure water thoroughly, the electrode was modified with 20 μLAuNPs-S2 for 2 h to form the "off" state. After that, 20 μL above intermediate DNA which linear correlated with target miRNA-141 was dipped onto the electrode for 2 h to adjust the distance between CdS:Mn QDs and AuNPs, which obtained a significantly increased ECL signal ("super on" state) because that the CdS:Mn QDs could excite the surface plasma resonance of AuNPs comparing to the "on" state. ECL measurement of the designed biosensor was carried out in 2 mL PBS which contained 0.01 M $S_2O_8^{2-}$ base solution. Finally, 20 μL of 1×Lambda exonuclease reaction buffer which contained 5 U Lambda exonuclease was incubated onto the modified electrode at 37 ºC for 1 h to hydrolyse the intermediate DNA, leading to a regeneration of the biosensor.

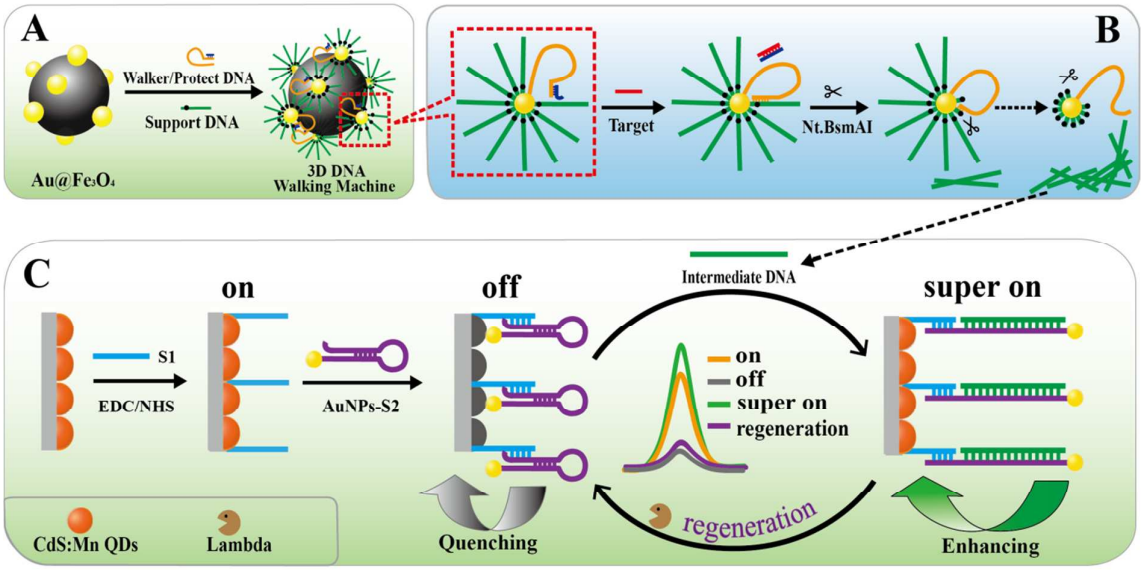

Scheme 1. Preparation process of the 3D DNA walking machine **(A)**, principles of the 3D DNA walking machine for target conversion **(B)** and schematic diagram of the "on-off-super on" ECL biosensor **(C)**.

RESULTS AND ANALYSIS

TEM characterizing of CdS:Mn QDs and AuNPs. To verify the fundamental of proposed biosensor, the prepared CdS:Mn QDs and AuNPs were characterized by transmission electron microscope (TEM). As shown in Figure 1A, the morphologies of CdS:Mn QDs presented the globular structure with average size about 5.0 nm. The dispersive and uniform AuNPs also showed globular structures with size of 4.2 ± 1.0 nm as Figure 1B. All the characterization results were consistent with the previous work,[22] indicating the successful preparation of CdS:Mn QDs and AuNPs.

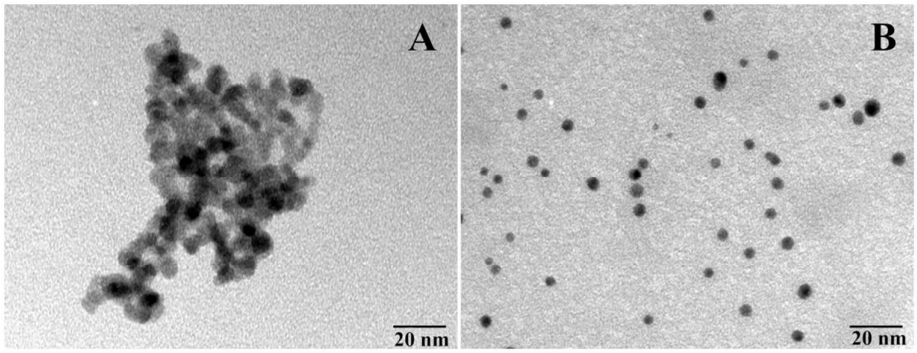

Figure 1. TEM of the CdS:Mn QDs **(A)** and AuNPs **(B).**

EIS and ECL characterization of the biosensor. Fabrication process of the biosensor was verified by electrochemical impedance spectroscopy (EIS). As shown in Figure 2A, the electron transfer resistance (*Ret*) of CdS:Mn QDs sensing platform (curve b) was significantly increased comparing with that of the bare GCE (curve a), which indicated the successfully assembling of CdS:Mn QDs. When S1 was cross-linked on the electrode surface, an increased *Ret* could be observed because of the negatively charged phosphate backbone of DNA which attenuated the electron transfer (curve c). After the assembly of AuNPs-S2, an increased *Ret* could be seen due to the dominant of S2 (long chain DNA) (curve d). As expected, the *Ret* kept increasing with the modification of intermediate DNA, proving the successfully pairing of dsDNA (curve e). However, once the Lambda exonuclease was introduced, a reduced *Ret* was clearly observed, which was attributed to the ablation of intermediate DNA (curve f). Notably, the *Ret* of curve f was similar to curve d, indicating that the Lambda exonuclease ablated the intermediate DNA to reduce the negatively charged phosphate backbone extremely.

To further verify the rationale of proposed sensing strategy, ECL was also employed to confirm the successful construction of the "on-off-super on" regenerated biosensor. As seen in Figure 2B, the biosensor had a strong ECL response with the modification of CdS:Mn QDs

("on" state). After AuNPs-S2 was introduced, a sharply reduced ECL response was observed due to the Förster energy transfer between CdS:Mn QDs and AuNPs ("off" state). In the following step, the intermediate DNA pared with AuNPs-S2 to form a dsDNA, which stretched the distance between AuNPs and CdS:Mn QDs to excite the surface plasmon resonance, leading to a significant enhancement of ECL response ("super on" state). As our expectation, the "super on" state which showed a higher ECL response than that of the "on" state is promising in increasing the sensitivity, and further achieving the ultrasensitive detection. Finally, a sharp reduction of ECL response was observed ("regenerate" state), along with the addition of Lambda exonuclease which ablated the intermediate DNA from 5′-3′ to restore the remaining AuNPs-S2 through the proximity ligation assay. The AuNPs got closer to the CdS:Mn QDs, leading to a quenching of ECL emission again. Impressively, the "regenerate" state had similar ECL value as the "off" state which verified the successful regeneration of the biosensor.

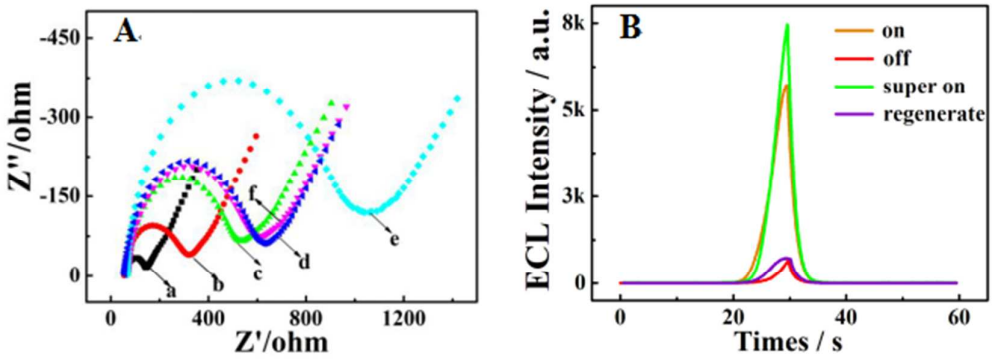

Figure 2. (A) EIS diagram of the electrode in the process (a. Bare GCE, b. GCE/CdS:Mn QDs, c. GCE/CdS:Mn QDs/S1, d. GCE/CdS:Mn QDs/S1/Au @ S2, e. GCE/CdS:Mn QDs/S1/Au @ S2/intermediate DNA, f. GCE/CdS:Mn QDs/S1/Au @ S2/intermediate DNA/Lambda Enzyme); **(B)** ECL intensity - time curves of the constructed process of the "on-off-super on" regenerated biosensor.

Optimal conditions of the ECL biosensor. Optimal conditions such as cleaving time of

Nt.BsmAI nicking exonuclease and the recovery time of biosensor were investigated to maximize the sensitivity and efficiency of our method. As shown in Figure 3A, when the cleaving time of Nt.BsmAI nicking exonuclease shifted from 40 to 140 min, the ECL response increased and reached the maximum at 120 min. Hence, 120 min was chosen as the appropriate experimental cleavage time. And Figure 3B showed the influence of recovery time towards biosensor. With the Lambda exonuclease cleaving time increasing at the range from 0 to 70 min, the ECL response decreased accordingly and reached a platform at 60 min, which indicated that the best regeneration result could be achieved at this time. Therefore, the cleaving time of Lambda exonuclease in this experiment was chosen as 60 min.

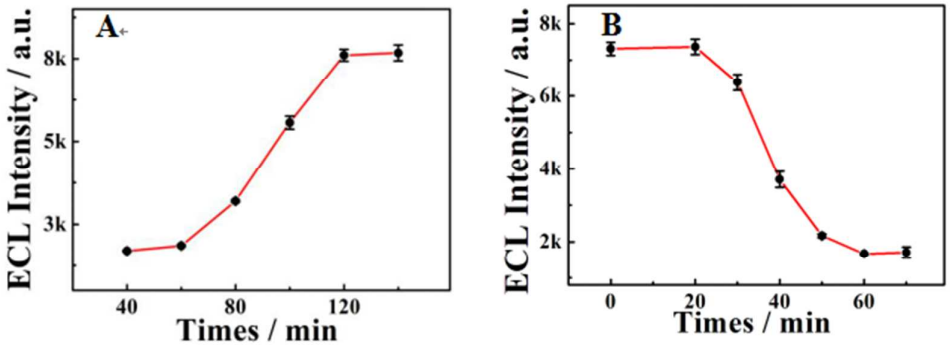

Figure 3. Influence of Nt.BsmAI nicking exonuclease cleaving time **(A)** and Lambda exonuclease cleaving time **(B)** on ECL intensity.

ECL performance of the biosensor. In order to further explore the quantitative accuracy of our system, the biosensor was applied for quantitative detection of miRNA-141 under the optimal condition. When the concentrations of miRNA-141 increased, stronger ECL responses were detected. The ECL signal showed a good liner relationship with the logarithm of miRNA-141 concentration which is shown in Figure 4. The linear regression equation is $I = 9319.08 + 2719.33 \lg c$ with the concentrations of miRNA-141 ranging from 10 fM to 100

pM (*I* is a symbol of ECL intensity and *c* is a symbol of the concentration of miRNA-141). The limit of detection (LOD) is 3.3 fM (LOD = 3 S_B/m, where *m* is the slope of the corresponding calibration curve and S_B is the standard deviation of the blank).[23] With such a lower detection limit, the ECL biosensor is more sensitive compared to other existing miRNA detection methods (Table 1), which showed a more effective way for quantifying miRNA-141.

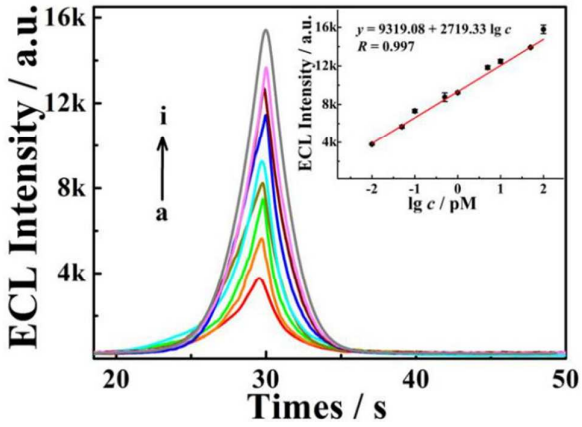

Figure 4. Cathodic ECL response of the designed biosensor in the presence of different concentrations of miRNA-141: 10 fM, 0.05 pM, 0.1 pM, 1 pM, 5 pM, 10 pM, 50 pM and 100 pM. Inset shows a calibration plot of the miRNA analysis.

Table 1. Comparison of the Existing MiRNA Detection Methods with Our Work

methods	detection strategy	detection limit	dynamic range	references
fluorescence	3D walker	300 fM	0.3 pM to 100 pM	19
fluorescence	Strand Displacement Amplification	50 nM	0.05 μM to 2.5 μM	24
ECL	1D walker	190 fM	0.5 pM to 10 nM	25
fluorescence	2D walker	58 fM	100 fM to 1 nM	26
ECL	3D walker	3.3 fM	10 fM to 100 pM	This work

Stability, reproducibility, selectivity and regenerability of the miRNA biosensor.

Furthermore, the stability, reproducibility and selectivity were essential elements for ECL assay which fully reflected the value of the sensor. As shown in Figure 5A, the evaluation of miRNA-141 (0.1 pM) was scanned under 10 consecutive cycles of cyclic potential, and almost no obvious changes of the ECL response could be observed, which indicated a good stability of the method. By evaluating variation coefficients (ECL signal) of three duplicate measurements, the reproducibility of ECL biosensor was evaluated and the relative standard deviation (RSD) was less than 5%. On the other hand, miRNA-141 and other interference miRNA sequences were used for selectivity investigation, and the result is prompted as Figure 5B. The significant enhancement of ECL intensity could be observed when miRNA-141 is presented, no matter a pure target solution or a mixture containing the target. When the other miRNAs were under the experiment condition, ECL responses were almost the same as that of the blank test. These results indicated the high selectivity of our sensing method. Notably, as shown in Figure 5C, when Lambda exonuclease was incubated at 37 °C for 1 h, the biosensor could be regenerated and was stable enough to detect miRNA-141 over five times. With many advantages such as saving operation time and improving the possibility of clinical application, the regenerability was another appealing innovation in this system.

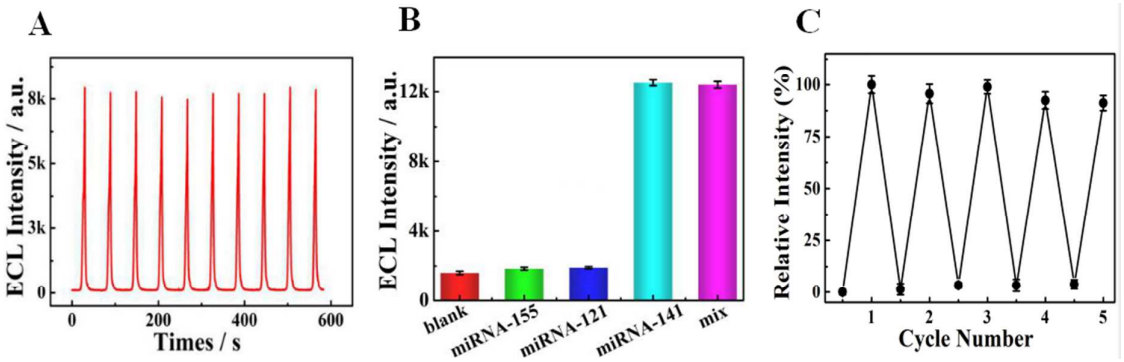

Figure 5. (A) Stability of the ECL biosensor with 0.1 pM miRNA-141under detected for 10 cycles over 590 s. **(B)** Selectivity analysis of the biosensor (blank, 100 pM miR-155, 100 pM miR-121, 10 pM

miRNA-141 and a mixture of 100 pM miR-155, 100 pM miR-121 and 10 pM miRNA-141). **(C)** Regeneration capability of the biosensor with 0.5 pM miRNA-141 over five cycle reuses.

Application. To further investigate the practical applicability of our method, miRNA-141 was detected in biological cell lysates of 22 Rvl human prostate cancer and Hela cervical cancer cell. As presented in Figure 6A, ECL signal of the biosensor with Rvl cells lysate accordingly increased with the number of cells in the lysate increasing from 0 to 100000. However the biosensor with Hela cells cells lysate had almost negligible ECL changes compared to that of the blank test even at a high number of 100000 cells. The results were consistent with previous studies for a relatively high expression of miRNA-141 in the 22 Rvl cells and a low expression of miRNA-141 in the HeLa cells.[27] Also, the ECL intensity showed a good linear relationship with the logarithms of 22 Rvl cells counts as presented in Figure 6B. linear equation $y = -926.09 + 2943.07 \lg N$ ($R = 0.996$, y is a symbol of ECL intensity and N is a symbol of the 22 Rvl cells counts) and the detection limit of 12 cells. From these experiment results, our proposed method had shown a good potentiality in quantifying miRNA of cells and clinical diagnostics of cancers.

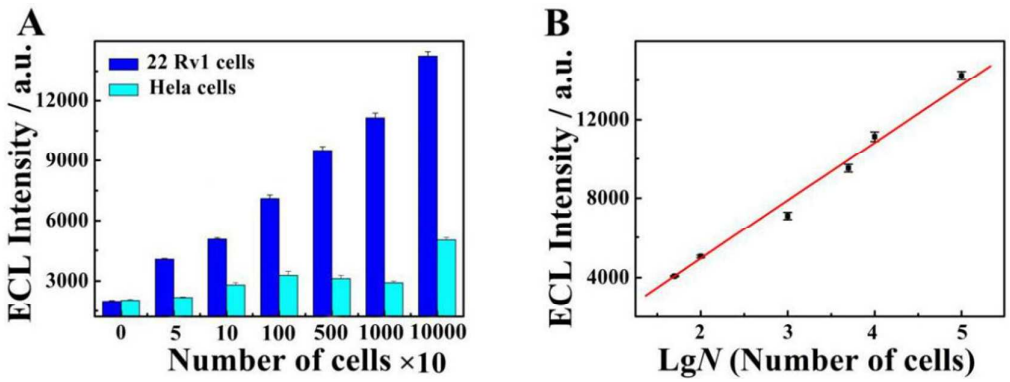

Figure 6. (A) ECL response of biosensor with different number of 22 Rvl and HeLa cancer cell lysates. **(B)** a calibration plot of the 22 Rvl cancer cells analysis.

CONCLUSIONS

In conclusion, on the basis of 3D DNA walking machine induced signal amplification and distance-based energy transfer induced “on-off-super on” strategy, an ECL biosensor was constructed for ultrasensitive miRNA-141 detection. Main characteristics and advantages were as follows. Firstly, the 3D DNA walking machine was introduced in the ECL system for target conversion, showing a high assembly efficiency and resulting in an excellent signal amplification, which were hundreds times better than that of the common 1D or 2D Walker. Besides, the skillfully designed "on-off-super on" strategy according to distance-based energy transfer between CdS:Mn QDs and AuNPs not only reduced the background signal to a sensitive detection of miRNA, but also guaranteed the selectivity. Lastly, the biosensor could be regenerated owing to the hydrolyzing of the Lambda exonuclease toward the dsDNA, resulting in the restore of hairpin structure of AuNPs-S2, which has the advantages of saving cost, reducing testing time compared to the conventional disposable sensor, benefiting the clinical detection of early diagnosis for cancer tumors. Considering these advantages, the well-designed biosensor has the promise for ultrasensitive detection of various tumor markers.

AUTHOR INFORMATION

* Corresponding authors

Tel.: +86 23 68252277, fax: +86 23 68253172.

E-mail addresses: hjwang@swu.edu.cn (H. J. Wang); yuanruo@swu.edu.cn (R. Yuan).

Notes

The authors declare no competing financial interest.

ACKNOWLEDGMENT

This work was financially supported by the National Natural Science Foundation of China (21675129, 51473136 and 21575116), the Fundamental Research Funds for the Central Universities (XDJK2016E055 and XDJK2017C023), and the China Postdoctoral Science Foundation (2016 M602626).

SUPPORTING INFORMATION AVAILABLE

Supporting Information mainly contains reagents and materials (Table S-1) and instrumentation. Optimal conditions of the ECL biosensor (Figure S1), PAGE analysis (Figure S2), characterization of $Au@Fe_3O_4$ (Figure S3) and ECL energy transfer between AuNPs and CdS:Mn QDs (Figure S4).

REFERENCES

(1) Mahiben M.; Johnathan W.; Mohd N. A.; Callum W.; Raghib A.; Richard S.; Thomas Z.; Rifat A. *Lancet* **2016**, *388*, 684-695.

(2) Lin S. B.; Gregory R. I. *Nat. Rev. Cancer* **2015**, *15*, 321-333.

(3) Hou T.; Li W.; Liu X. J.; Li F. *Anal. Chem.* **2015**, *87*, 11368-11374.

(4) Liu C.; Liu R. F.; Zhang D. X.; Deng Q.; Liu B. G.; Chao H. P.; Rycaj K.; Takata Y; Lin K.; Lu Y.; Zhong Y.; Krolewski J.; Shen J. J.; Tang D. G. *Nat. Commun.* **2017**, *8*, 14270-14283.

(5) Jou A. F.; Lu C. H.; Ou Y. C.; Wang S. S.; Hsu S. L.; Willner I.; Ho J. A. *Chem. Sci*. **2015**, *6*, 659-665.

(6) Jung S.; Kim J.; Lee D. J.; Oh E. H.; Lim H.; Kim K. P.; Choi N.; Kim T. S.; Kim S. K. *Sci. Rep*. **2016**, *6*, 22975-22981.

(7) Liao R.; He K.; Chen C. Y.; Chen X. M.; Cai C. Q. *Anal. Chem*. **2016**, *88*, 4254-4258.

(8) Li Y.; Zhang C. Y. *Anal. Chem*. **2012**, *84*, 5097-5102.

(9) Jin S.; Furtaw M. D.; Chen H. X.; Lamb D. T.; Ferguson S. A.; Arvin N. E.; Dawod M.; Kennedy R. T. *Anal. Chem*. **2016**, *88*, 6703-6710.

(10) Li L. L.; Chen Y.; Zhu J. J. *Anal. Chem.* **2017**, *89*, 358-371.

(11) Hesariand M.; Ding Z. F. *J. Electrochem. Soc.* **2016**, 163, H3116-H3131.

(12) Liu Z. Y.; Qi W. J.; Xu G. B. *Chem. Soc. Rev.* **2015**, *44*, 3117-3142.

(13) Mohsen M. G.; Kool E. T. *Acc. Chem. Res*. **2016**, *49*, 2540-2550.

(14) Russell C.; Roy S.; Ganguly S.; Qian X. Y.; Caruthers M. H.; Nilsson M. *Anal. Chem*. **2015**, *87*, 6660-6666.

(15) Nicholas A. M.; William G. E.; Austin H. N.; Frederick H. R. *Anal. Chem*. **2017**, *89*, 728-735.

(16) Marx V. *Nat. Methods* **2015**, *12*, 393-397.

(17) Cha T. G.; Pan J.; Chen H. R.; Robinson H. N.; Li X.; Mao C. D.; Choi J. H. *J. Am. Chem. Soc.* **2015**, *137*, 9429-9437.

(18) Liu M. H.; Cheng J.; Tee S. R.; Sreelatha S.; Loh I. Y.; Wang Z. S. *ACS Nano* **2016**, *10*, 5882-5890.

(19) Yang X. L.; Tang Y. A.; Mason S. D.; Chen J. B.; Li F. *ACS Nano* **2016**, *10*, 2324-2330.

(20) Du X. J.; Jiang D.; Hao N.; Liu Q.; Qian J.; Dai L. M.; Mao H. P.; Wang K. *Chem. Commun*. **2015**, *51*, 11236-11239.

(21) Jiang X. Y.; Wang H. J.; Wang H. J.; Yuan R.; Chai Y. Q. *Anal. Chem*. **2016**, *88*, 9243-9250.

(22) Shan Y.; Xu J. J.; Chen H. Y. *Chem. Commun*. **2009**, *1*, 905-907.

(23) Radi A.; Sánchez J. L. A.; Baldrich E.; O'Sullivan C. K. *J. Am. Chem. Soc.* **2006**, *128*, 117-124.

(24) Zhang J. P.; Li C.; Zhi X.; Ramon G. A.; Liu Y. L.; Zhang C. L.; Pan F.; Cui D. X. *Anal. Chem*. **2016**, *88*, 1294-1302.

(25) Chen Y.; Xiang Y.; Yuan R.; Chai Y. Q. *Nanoscale* **2015**, *7*, 981-986.

(26) Wang L. D.; Deng R. J.; Li J. H. *Chem. Sci.* **2015**, *6*, 6777-6782.

(27) Zhou W. J.; Liang W. B.; Li X.; Chai Y. Q.; Yuan R.; Xiang Y. *Nanoscale*, **2015**, *7*, 9055-9061

TOC graphic